The Journal of Immunology

Targeting Peroxiredoxin 1 by a Curcumin Analogue, AI-44, Inhibits NLRP3 Inflammasome Activation and Attenuates Lipopolysaccharide-Induced Sepsis in Mice

Wen Liu, Wenjie Guo, Yongcheng Zhu, Shuang Peng, Wei Zheng, Chao Zhang, Fenli Shao, Yuyu Zhu, Nan Hang, Lingdong Kong, Xiangbao Meng, Qiang Xu and Yang Sun

J Immunol 2018; 201:2403-2413; Prepublished online 5 September 2018;
doi: 10.4049/jimmunol.1700796
http://www.jimmunol.org/content/201/8/2403

The Journal of Immunology is published twice each month by
The American Association of Immunologists, Inc.,
1451 Rockville Pike, Suite 650, Rockville, MD 20852

Print ISSN: 0022-1767 Online ISSN: 1550-6606.

Targeting Peroxiredoxin 1 by a Curcumin Analogue, AI-44, Inhibits NLRP3 Inflammasome Activation and Attenuates Lipopolysaccharide-Induced Sepsis in Mice

Wen Liu,*,[1] Wenjie Guo,*,[1] Yongcheng Zhu,* Shuang Peng,* Wei Zheng,* Chao Zhang,[†] Fenli Shao,* Yuyu Zhu,* Nan Hang,* Lingdong Kong,* Xiangbao Meng,[†] Qiang Xu,* and Yang Sun*

Aberrant activation of the NLRP3 inflammasome contributes to the onset and progression of various inflammatory diseases, making it a highly desirable drug target. In this study, we screened a series of small compounds with anti-inflammatory activities and identified a novel NLRP3 inflammasome inhibitor, AI-44, a curcumin analogue that selectively inhibited signal 2 but not signal 1 of NLRP3 inflammasome activation. We demonstrated that AI-44 bound to peroxiredoxin 1 (PRDX1) and promoted the interaction of PRDX1 with pro–Caspase-1 (CASP1), which led to the suppression of association of pro-CASP1 and ASC. Consequently, the assembly of the NLRP3 inflammasome was interrupted, and the activation of CASP1 was inhibited. Knockdown of PRDX1 significantly abrogated the inhibitory effect of AI-44 on the NLRP3 inflammasome. Importantly, AI-44 alleviated LPS-induced endotoxemia in mice via suppressing NLRP3 inflammasome activation. Taken together, our work highlighted PRDX1 as a negative regulator of NLRP3 inflammasome activation and suggested AI-44 as a promising candidate compound for the treatment of sepsis or other NLRP3 inflammasome-driven diseases. ***The Journal of Immunology*****, 2018, 201: 2403–2413.**

Sepsis is defined as life-threatening organ dysfunction due to a dysregulated host response to infection (1, 2). Despite the implementation of goal-directed care, poor prognosis and high mortality still remain when it is associated with organ dysfunction, hypoperfusion, or hypotension. LPS initiates an excessive host response associated with a nonresolving systemic inflammatory response syndrome, contributing to the pathogenesis of sepsis, including the release of proinflammatory mediators such as IL-1β (3–5).

The inflammasome pathway has been reported to be involved in the inflammatory response in sepsis (6). The NLRP3 inflammasome is one kind of germline-encoded pattern recognition receptor participating in the innate immune system to initiate downstream inflammatory cascades (7). Two signals are required for the classical activation of the NLRP3 inflammasome. For signal 1, LPS activates TLR4 and promotes activation of NF-κB and transcriptions of pro–IL-1β and pro–IL-18. For signal 2, activators, including damage-associated molecular patterns, initiate the assembly of NLRP3 inflammasome complexes, leading to Caspase-1 (CASP1) activation. NLRP3 inflammasome activation serves as a platform for maturation of pro–IL-1β and pro–IL-18 (8). Although several types of NLRP3 inflammasome inhibitors have been developed and exploited to treat inflammation-associated diseases such as sepsis, obesity, and colitis-associated cancer (9–15), compounds with more potential activity, selectivity, and druggability still remain to be discovered.

Recent studies on networks of the NLRP3 inflammasome mainly focus on the regulation of signal 2 activation. It was reported that tyrosine phosphatase SHP2 (16) and leucine-rich repeat Fli-I–interacting protein 2 (LRRFIP2) (17) negatively regulated NLRP3 inflammasome activation, whereas cathepsin B (18) could directly activate the NLRP3 inflammasome. Our study found that curcumin analogue AI-44 specifically bound to peroxiredoxin 1 (PRDX1) and suppressed the activation of the NLRP3 inflammasome, alleviating LPS-induced murine endotoxemia. Our work contributes to the finding of a new regulator of the NLRP3 inflammasome and provides a new candidate compound for the treatment of NLRP3 inflammasome–associated disease.

Materials and Methods

Mice

Six- to eight-week-old female C57BL/6 mice were purchased from Model Animal Research Center of Nanjing University (Nanjing, China). NLRP3 knockout mice were presented as a gift from Prof. Rongbin Zhou (University

*State Key Laboratory of Pharmaceutical Biotechnology, Department of Biotechnology and Pharmaceutical Sciences, School of Life Sciences, Nanjing University, Nanjing 210023, China; and [†]State Key Laboratory of Natural and Biomimetic Drugs, Department of Chemical Biology, School of Pharmaceutical Sciences, Peking University, Beijing 100191, China

[1]W.L. and W.G. contributed equally to this work.

ORCIDs: 0000-0001-8506-3905 (W.G); 0000-0002-0514-7904 (F.S.); 0000-0002-6885-4083 (Y.Z.); 0000-0002-7445-7674 (N.H.); 0000-0003-3418-9975 (X.M.); 0000-0003-1425-0089 (Y.S.).

Received for publication June 5, 2017. Accepted for publication August 3, 2018.

This work was supported by the National Natural Science Foundation of China Grants 81673436, 81673437, 81872877, 81330079, and 81573272, the Mountain-Climbing Talents Project of Nanjing University, and the open fund of the State Key Laboratory of Pharmaceutical Biotechnology, Nanjing University, Nanjing, China (Project KF-GN-201703).

Address correspondence and reprint requests to Prof. Yang Sun, Prof. Qiang Xu, or Assoc. Prof. Xiangbao Meng, School of Life Sciences, Nanjing University, 163 Xianlin Avenue, Nanjing 210023, China (Y.S. and Q.X.) or School of Pharmaceutical Sciences, Peking University, 38 Xueyuan Road, Haidian District, Beijing 100191, China (X.M.). E-mail addresses: yangsun@nju.edu.cn (Y.S.), molpharm@163.com (Q.X.), or xbmeng@bjmu.edu.cn (X.M.)

The online version of this article contains supplemental material.

Abbreviations used in this article: AI-44–Biotin, biotin-tagged AI-44; ALT, alanine transaminase; Andro, andrographolide; AST, aspartate aminotransferase; BMDM, bone marrow–derived macrophage; CASP1, Caspase-1; CETSA, cellular thermal shift assay; GasD, gasdermin D; LDH, lactate dehydrogenase; MSU, monosodium urate; PRDX1, peroxiredoxin 1; ROS, reactive oxygen species.

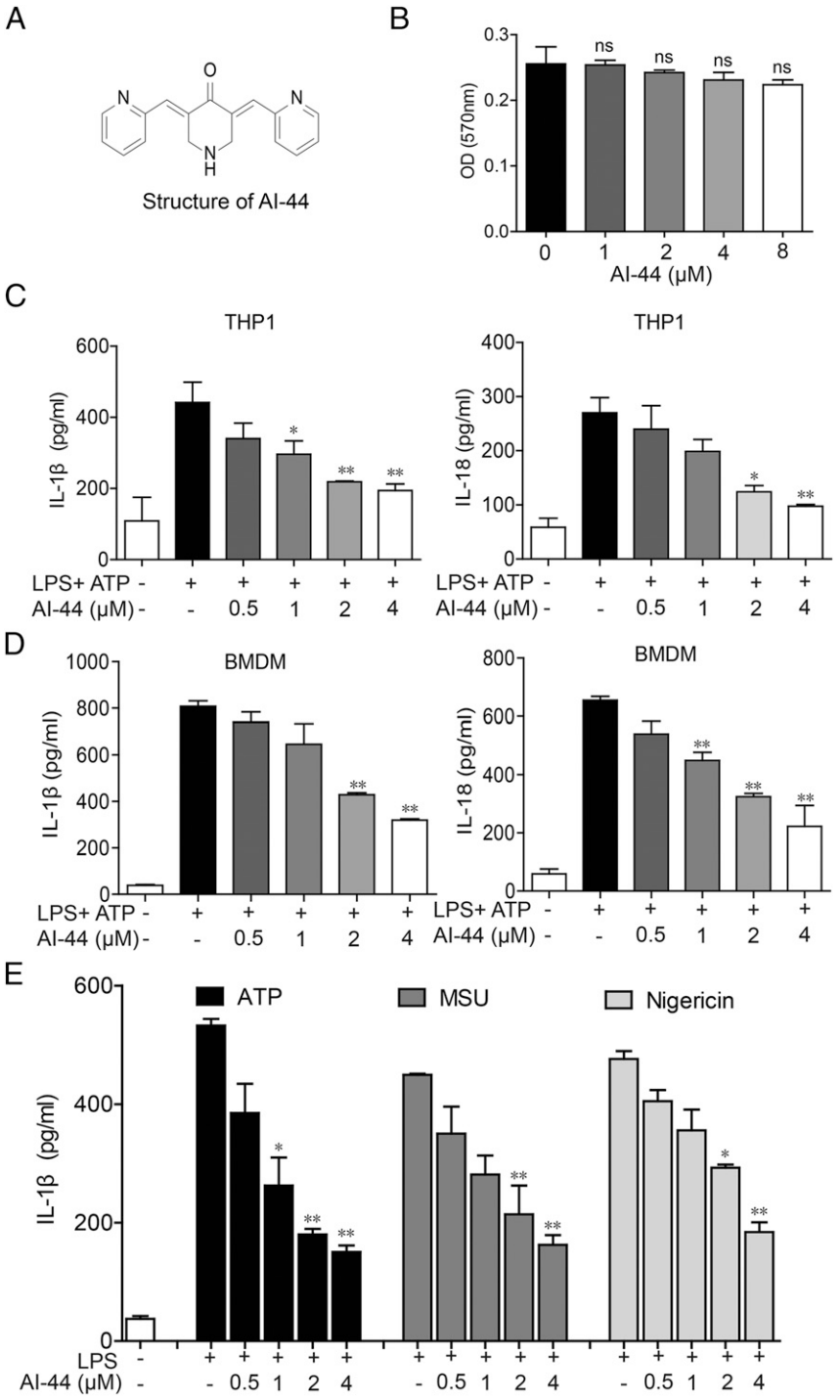

FIGURE 1. Curcumin analogue AI-44 suppresses IL-1β production in macrophage. (**A**) Chemical structure of AI-44. (**B**) PMA-differentiated THP1 cells were treated with AI-44 for the indicated doses. After 24 h, cell availability was determined by MTT assay. (**C**) PMA-differentiated THP1 cells and (**D**) BMDM were stimulated with 100 ng/ml LPS for 3 h, followed by 1 h AI-44 incubation for the indicated doses, and then treated with 5 mM ATP for 1 h. IL-1β and IL-18 in the supernatant were analyzed by ELISA. (**E**) PMA-differentiated THP1 cells were stimulated with 100 ng/ml LPS for 3 h, followed by 1 h AI-44 incubation for the indicated doses, and then treated with ATP (5 mM, 1 h), MSU (500 μg/ml, 2 h), or nigericin (10 μM, 2 h), respectively. IL-1β in the supernatant was analyzed by ELISA. Data are presented as mean ± SEM of three independent experiments. $*p < 0.05$, $**p < 0.01$ versus vehicle control.

of Science and Technology of China, Hefei, China). Animal welfare and experimental procedures were carried out strictly in accordance with the Guide for the Care and Use of Laboratory Animals (National Institutes of Health) and the related ethical regulations of our university. All efforts were made to minimize animals' suffering and to reduce the number of animals used.

Reagents

A series of AI compounds were synthesized by Prof. Xiangbao Meng (School of Pharmaceutical Sciences, Peking University) with the detailed information in Supplemental Fig. 1. Compounds were dissolved at a concentration of 30 mM in 100% DMSO as a stock solution (stored at −20°C) and diluted with medium when used. The final concentration of DMSO did not exceed 0.1% throughout the study (all the control groups are composed of 0.1% DMSO). LPS from *Escherichia coli* (0111:B4), PMA, and ATP were purchased from Sigma-Aldrich (St. Louis, MO). The lactate dehydrogenase (LDH) kit and alanine transminase (ALT) and aspartate aminotransferase (AST) activity assay kits were purchased from Nanjing Jiancheng Bioengineering Institute (Nanjing, China). RPMI 1640, FBS, Alexa Fluor 546 Donkey anti-Rabbit IgG, and Alexa Fluor 488 Donkey anti-Mouse IgG (H + L) were purchased from Life Technologies (Carlsbad, CA). Anti-CD11b–FITC was purchased from eBioscience (San Diego, CA). Anti–phospho-p65 and anti-p65 were purchased from Cell Signaling Technology (Beverly, MA). Anti-NLRP3 and anti-CASP1 were purchased from Epitomics (Burlingame, CA). Anti-ASC and anti-PRDX1 were purchased from Santa Cruz Biotechnology (Santa Cruz, CA). Anti–gasdermin D (GasD) was purchased from Santa Cruz Biotechnology. ELISA kits for murine TNF-α, IL-1β, and IL-6 and human IL-1β were purchased from Dakewe Biotech (Beijing, China). All other chemicals were purchased from Sigma-Aldrich.

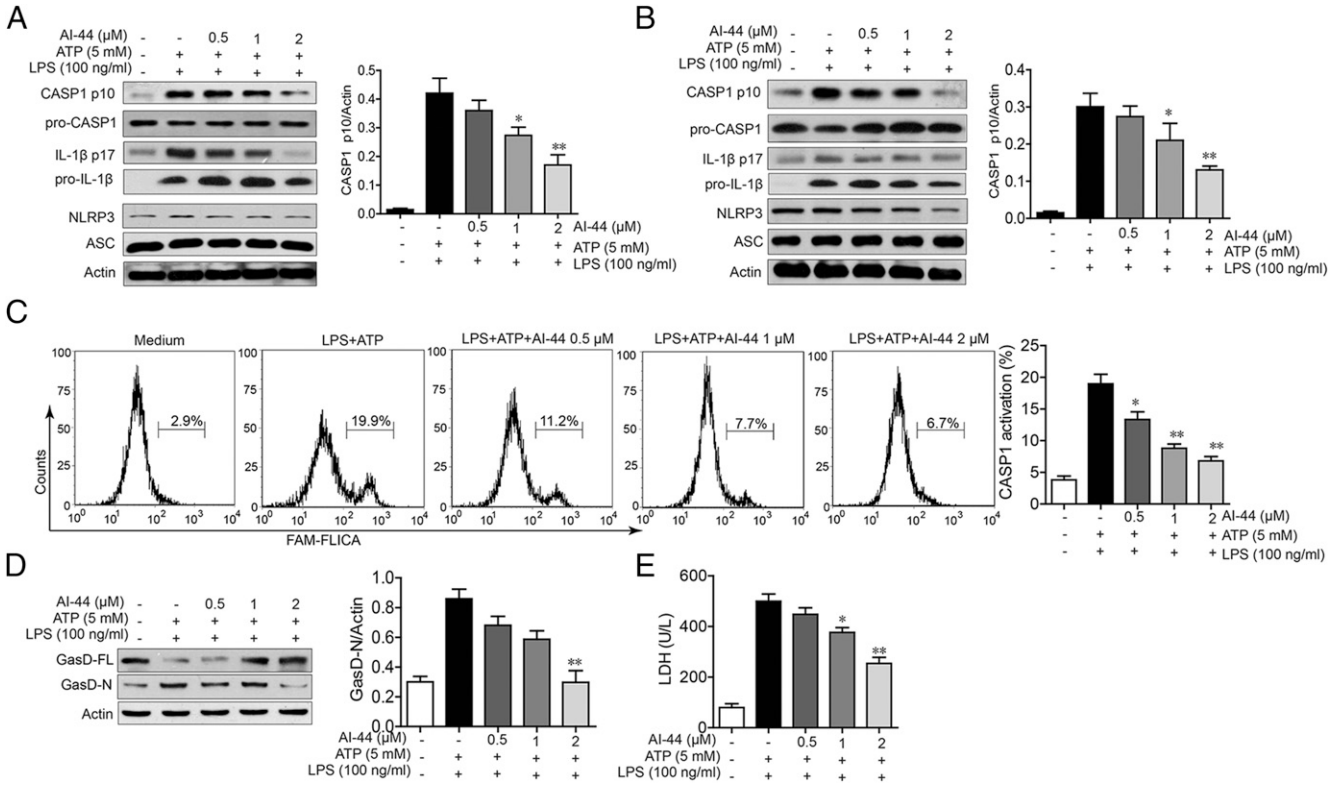

FIGURE 2. Curcumin analogue AI-44 inhibits CASP1 activation during NLRP3 inflammasome activation. PMA-differentiated THP1 cells (**A**) or BMDM (**B**) were incubated with 100 ng/ml LPS for 3 h, followed by indicated dose of AI-44 treatment for 1 h and then another 1 h of 5 mM ATP stimulation. Protein levels in the cell lysates were determined with indicated Abs by Western blot. PMA-differentiated THP1 cells were incubated with 100 ng/ml LPS for 3 h, followed by indicated dose of AI-44 treatment for 1 h and then another 1 h of 5 mM ATP stimulation. Cells were collected and stained with FAM FLICA and subjected for (**C**) flow cytometric analysis. GasD cleavage was determined with indicated Abs by (**D**) Western blot. (**E**) PMA-differentiated THP1 cells were incubated with 100 ng/ml LPS for 3 h, followed by indicated dose of AI-44 for 1 h and then another 1 h of 5 mM ATP. LDH level in the culture supernatant was examined. Data are presented as mean ± SEM of three independent experiments. $*p < 0.05$, $**p < 0.01$ versus vehicle control.

Cell culture

Human THP1 cell line was purchased from the Cell Bank of the Chinese Academy of Sciences (Shanghai, China) and maintained in RPMI 1640 medium, supplemented with 100 U/ml penicillin, 100 μg/ml streptomycin, and 10% FCS under a humidified 5% (v/v) CO_2 atmosphere at 37°C. Bone marrow–derived macrophage (BMDM) cells were isolated according to the following procedures. Bone marrow cells were isolated from C57BL/6 mice and cultured with DMEM supplemented with 10% FBS and 20 ng/ml GM-CSF (PeproTech, Rock Hill, NJ). Culture fluid was exchanged to fresh culture medium every 3 d. Under these conditions, adherent macrophages were obtained within 7–8 d. Cells were harvested and seeded on 24-well plates. After culture for 6 h without GM-CSF, the cells were used for the experiments as BMDM.

LPS-induced endotoxemia in mice and treatment

C57BL/6 mice were administered LPS at 20 mg/kg i.p. and survival was monitored continuously for 100 h ($n = 10$ per group). AI-44 (1, 3, or 10 mg/kg) was administered i.p. or andrographolide (Andro; 30 mg/kg) was administered intragastrically immediately after LPS injection. Serum was collected at 24 h after LPS administration to measure the levels of ALT, AST, and cytokines.

Cytokine analysis by ELISA

The levels of IL-1β, IL-6, and TNF-α in the serum or cell culture supernatant were quantified by an ELISA kit (Dakewe Biotech).

Immunofluorescence histochemistry

$CD11b^+$ macrophage infiltration analysis was performed on paraffin-embedded colonic tissue sections (5 μm). Briefly, the sections were deparaffinized, rehydrated, and washed in 1% PBS–Tween 20. Next, they were treated with 2% hydrogen peroxide, blocked with 3% goat serum, and incubated for 2 h at room temperature with anti-CD11b–FITC (1:100). The slides were then counterstained with DAPI for 2 min. The reaction was stopped by thorough washing in water for 20 min. Images were acquired by a confocal laser–scanning microscope (Olympus, Lake Success, NY). Settings for image acquisition were identical for control and experimental tissues.

Immunofluorescence cytochemistry

BMDM on coverslips were fixed in 4% paraformaldehyde, permeabilized with 0.5% Triton X-100 for 20 min, and blocked with 3% BSA for 30 min. Cells were immunostained with monoclonal anti-ASC together with anti-CASP1 Ab overnight. Next, Alexa Fluor 488–conjugated anti-mouse IgG and Alexa Fluor 594–conjugated anti-rabbit IgG (Life Technologies) were immunostained for 2 h. The coverslips were counterstained with DAPI and imaged with a confocal laser–scanning microscope (Olympus).

Western blot

The protein lysates were separated by 10% SDS-PAGE and subsequently electrotransferred onto a polyvinylidene difluoride membrane (Millipore, Bedford, MA). The membrane was blocked with 5% nonfat milk for 1 h at room temperature. The blocked membrane was incubated with the indicated primary Abs and then with an HRP-conjugated secondary Ab. Protein bands were visualized using a Western blotting detection system according to the manufacturer's instructions (Cell Signaling Technology).

Biotin pull-down assay

THP1 cell lysates were incubated with biotin, biotin-tagged AI-44 (AI-44–Biotin), or AI-44–Biotin plus AI-44 at 4°C for 12 h. The lysates were pulled down with streptavidin-conjugated beads (Softlink Soft Release Avidin Resin; Promega) at 4°C for another 4 h. After an extensive wash with PBS, the beads were boiled in 2× loading buffer (100 mM Tris-HCl [pH 6.8], 4% SDS, 1% bromophenol blue, 20% glycerol, and 2% 2-ME). Next, the supernatants were collected and subject to Western blot.

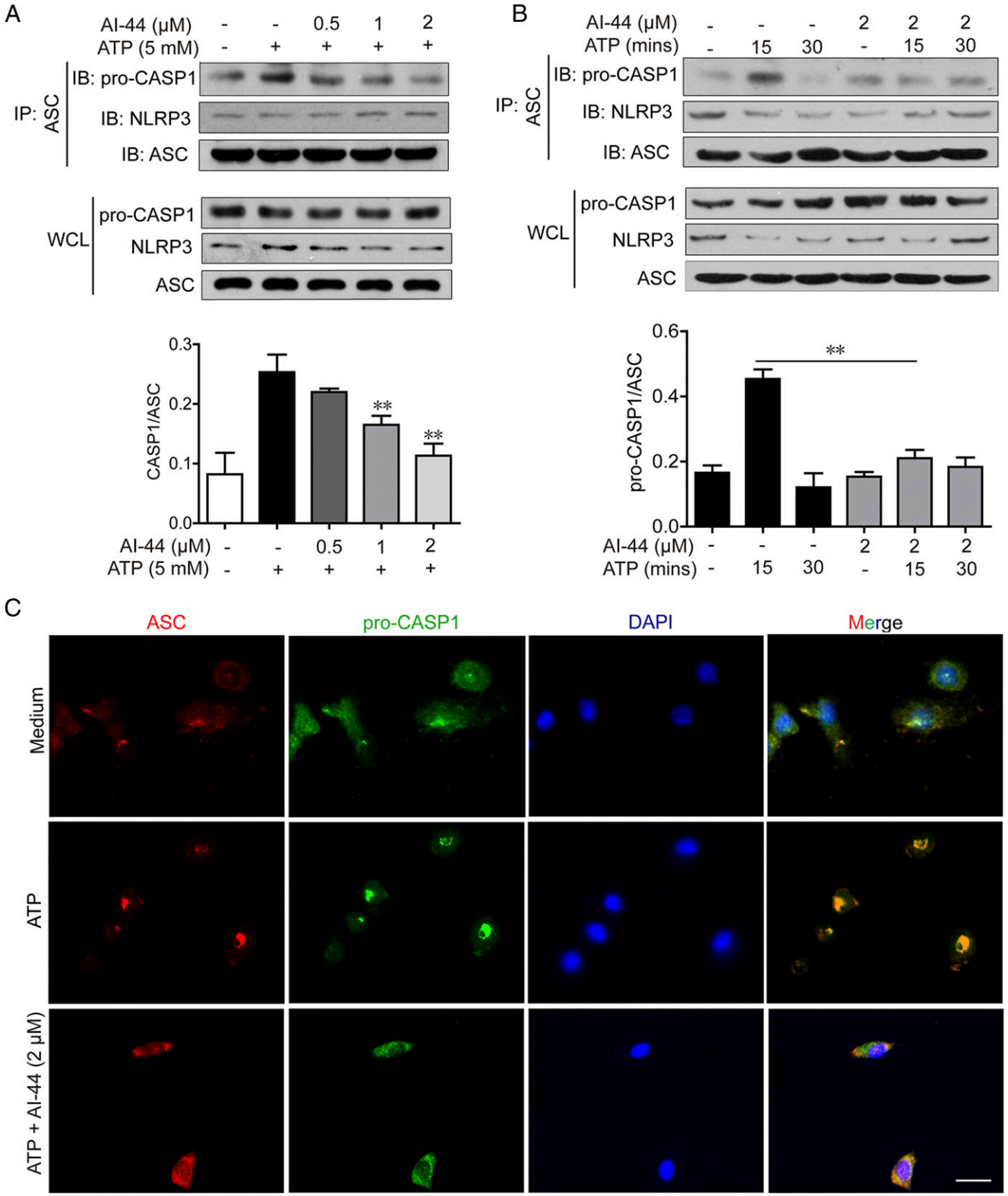

FIGURE 3. Curcumin analogue AI-44 interrupts the formation of NLRP3 inflammasome complex. (**A**) PMA-differentiated THP1 cells were incubated with 100 ng/ml LPS for 3 h, followed by indicated dose of AI-44 treatment for 1 h and then another 15 min of 5 mM ATP stimulation. Cell lysates were immunoprecipitated with anti-ASC Ab. (**B**) PMA-differentiated THP1 cells were incubated with AI-44 for 1 h and stimulated with 5 mM ATP for 15 or 30 min, respectively. Cell lysates were immunoprecipitated with anti-ASC Ab. (**C**) BMDM cells were incubated with 100 ng/ml LPS for 3 h, followed by indicated dose of AI-44 treatment for 1 h, and then stimulated with 5 mM ATP for 15 min. Colocalization of ASC and pro-CASP1 was determined by immunofluorescence. Scale bar, 10 μm. Data are presented as mean ± SEM of three independent experiments. $^{**}p < 0.01$.

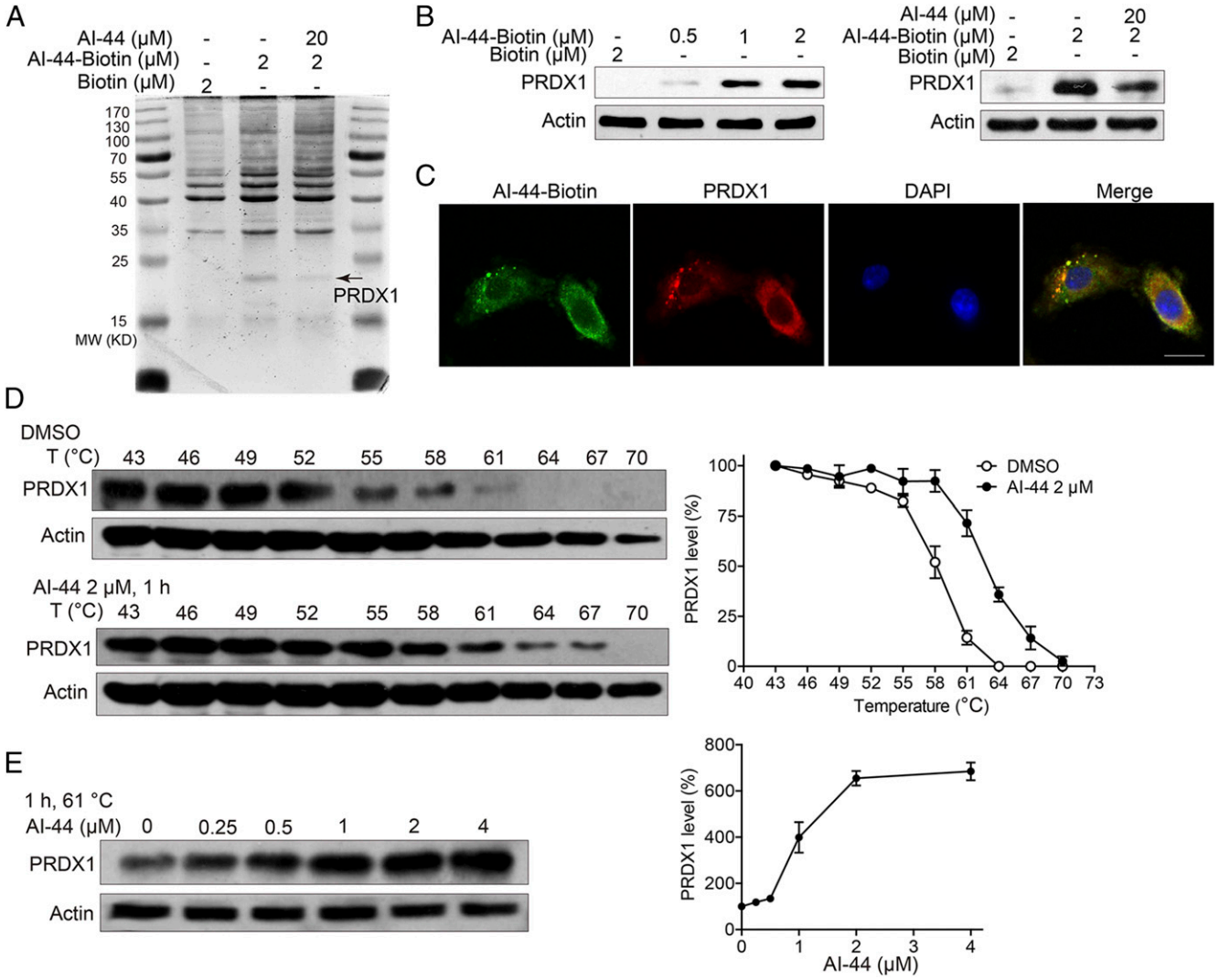

FIGURE 4. Curcumin analogue AI-44 targets PRDX1. THP1 cell lysates were incubated with biotin, number 2 AI-44–Biotin, or number 2 AI-44–Biotin plus AI-44 of indicated doses, respectively, for 12 h, and then cell lysates were immunoprecipitated with streptavidin-agarose beads. The pull-down protein was identified by (**A**) mass spectrometry or (**B**) Western blot. (**C**) Colocalization of AI-44 and PRDX1 in BMDM was determined by immunofluorescence. Scale bar, 10 μm. (**D**) THP1 cells were incubated with vehicle control or AI-44 (2 μM) for 1 h, then the cells were collected and subjected to CETSA. (**E**) THP1 cells were incubated with AI-44 (0, 0.25, 0.5, 1, 2, 4 μM) for 1 h, then the cells were collected and subjected to CETSA at the temperature of 61°C. Data shown are representative of three independent experiments.

Cellular thermal shift assay

THP1 cells were incubated with DMSO or AI-44 (2 μM) for 2 h, then the cells were collected and subjected to cellular thermal shift assay (CETSA) (19). Briefly, incubated cells were equally divided into 10 parts; each part was heated for 3 min under different temperatures (43, 46, 49, 52, 55, 58, 61, 64, 67, 70°C), then the heated cells were kept at −80°C for 12 h and transferred to room temperature for 5 min, and the whole sequence was repeated one more time. Next, cell lysates were extracted by centrifugation at 20,000× *g* for 20 min. PRDX1 expression was detected by Western blot.

Statistical analysis

Results were expressed as mean ± SEM of three independent experiments, and each experiment included triplicate sets. Data were statistically evaluated by one-way ANOVA, followed by Dunnett test between control group and multiple dose groups. A p value < 0.05 was considered statistically significant.

Results

AI-44 inhibits IL-1β secretion in macrophages

Previously, we reported that a benzo[*d*]imidazole derivate Fc11a-2 inhibited NLRP3 inflammasome activation and contributed to colitis improvement (20). Based on this lead compound, we synthesized a series of Fc11a-2 derivates, aiming to screen out more potent compounds. The structures and inhibitory activities on IL-1β of these compounds were shown in Supplemental Fig. 1. Compound AI-44 (Fig. 1A), a curcumin analogue with the highest inhibitory activity on IL-1β secretion, was selected for further study. As shown in Fig. 1B–D, AI-44 suppressed IL-1β as well as IL-18 secretion in BMDM and THP1-derived macrophages triggered by ATP without affecting cell viabilities. Moreover, AI-44 also inhibited IL-1β secretion stimulated by other danger signals such as monosodium urate (MSU) or nigericin in a dose-dependent manner (Fig. 1E). These results suggest that curcumin analogue AI-44 acts as a promising inhibitor for the NLRP3 inflammasome.

AI-44 suppresses the formation of the NLRP3 inflammasome

Next, we elucidated the activity characteristics of AI-44 against the inflammasome activation. Interestingly, AI-44 showed significant inhibitory effect on pro-CASP1 cleavage (Fig. 2A–C) but

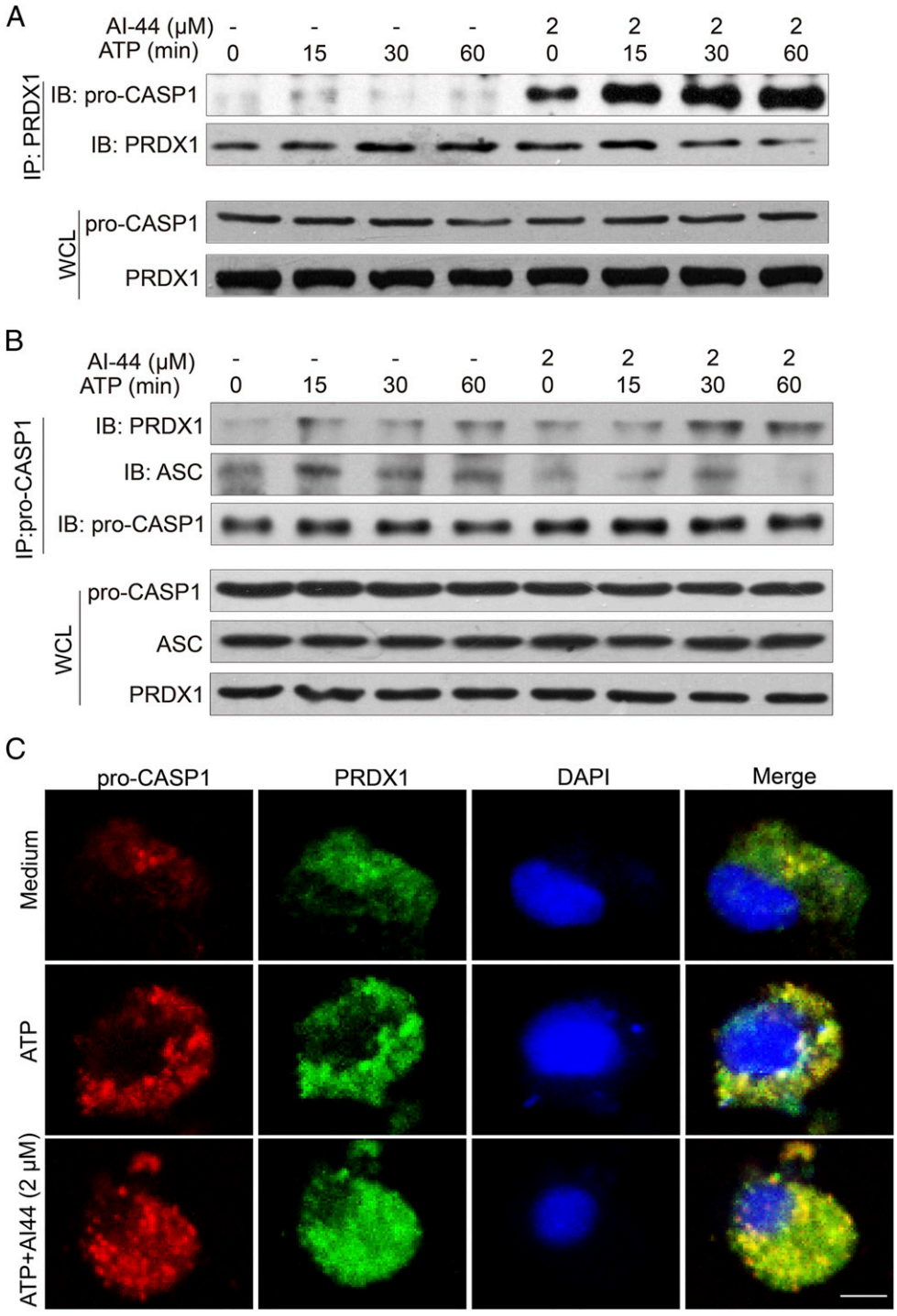

FIGURE 5. Curcumin analogue AI-44 promotes the interaction between pro-CASP1 and PRDX1. LPS-primed THP1 cells were treated with 2 μM AI-44 for 1 h, followed by 5 mM ATP stimulation for the indicated time. Cell lysates were immunoprecipitated with anti-PRDX1 (**A**) or anti–pro-CASP1 (**B**). One hundred nanograms per milliliter LPS-primed BMDM cells were treated with 3 μM AI-44 for 1 h, followed by 5 mM ATP stimulation for 10 min. Colocalization of pro-CASP1 and PRDX1 was determined by immunofluorescence assay (**C**). Scale bar, 10 μm. Data shown are representative of three independent experiments.

negligible effect on TNF-α production or NF-κB p65 activation (Supplemental Fig. 2A, 2B), suggesting the selectivity of AI-44 on its anti-inflammatory action. The cleavage of GasD and the release of LDH were also inhibited by AI-44 treatment. These results also hinted that AI-44 might selectively inhibit signal 2 but not signal 1 of NLRP3 inflammasome activation. It should be noted that AI-44 did not inhibit AIM2 activation induced by poly (dA:dT) in THP1-derived macrophages (Supplemental Fig. 2C).

As hypothesized, AI-44 interrupted the assembly of the NLRP3 inflammasome in a dose-dependent (Fig. 3A) and time-dependent (Fig. 3B) manner. Moreover, immunofluorescence analysis also showed that ASC–pro-CASP1 specks were remarkably reduced in AI-44–treated cells (Fig. 3C). These results suggest that AI-44 suppresses NLRP3 inflammasome activation via inhibiting the assembly of NLRP3–ASC–pro-CASP1 complex.

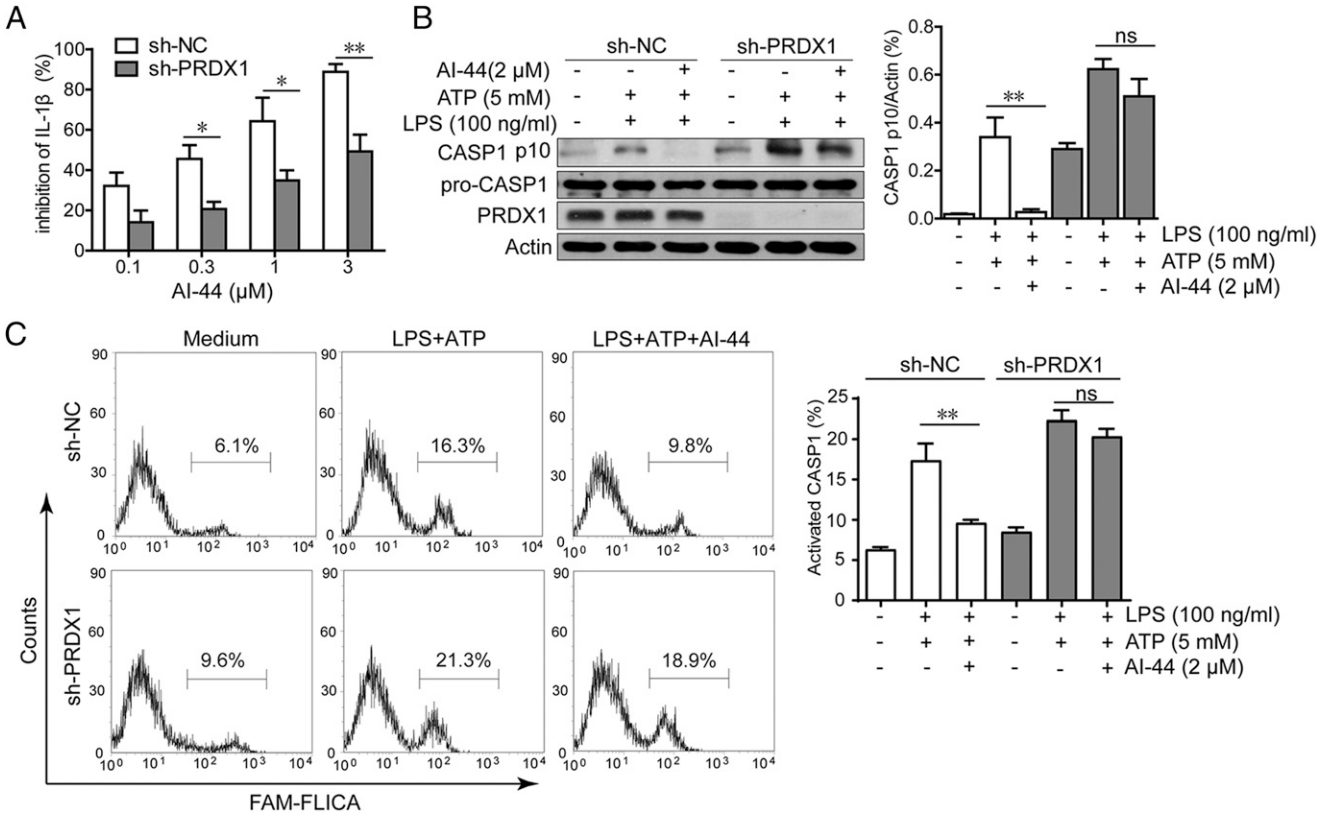

FIGURE 6. PRDX1 is required for inhibition of NLRP3 inflammasome activation by curcumin analogue AI-44. PRDX1 knockdown THP1 cells were generated by short hairpin RNA–PRDX1 (short hairpin RNA–negative control as control). PRDX1 knockdown THP1 cells were incubated with 100 ng/ml LPS for 3 h, followed by 2 μM AI-44 treatment for 1 h, and then treated with 5 mM ATP for 1 h. (**A**) IL-1β in the supernatant was determined by ELISA. (**B**) Protein levels in the cell lysates were determined with indicated Abs by Western blot. (**C**) Activation of CASP1 was examined by FAM FLICA staining and subjected to flow cytometric analysis. Data are presented as mean ± SEM of three independent experiments. $*p < 0.05$, $**p < 0.01$. ns, not significant.

AI-44 specifically targets PRDX1

To figure out the potential targets of AI-44 in macrophage, different arm lengths of biotin were conjugated to AI-44, and the one that showed comparable activity with AI-44 was chosen as bait for further investigation (Supplemental Fig. 3). For this purpose, number 2 AI-44–Biotin (structure shown in Supplemental Fig. 3) was selected as a useful probe for pull down assay (Fig. 4). As shown in Fig. 4A and 4B, number 2 AI-44–Biotin effectively pulled down PRDX1. This binding was competitively inhibited by higher concentrations of unlabeled AI-44, indicating that AI-44 directly targeted PRDX1. Moreover, immunofluorescence staining also demonstrated that number 2 AI-44–Biotin colocalized with PRDX1 in the cytoplasm of the macrophages (Fig. 4C).

To further confirm that AI-44 targets PRDX1, we performed a CETSA, a recently described method that allows rapid and simple assessment of target engagement of drugs in a cellular context. As shown in Fig. 4D, PRDX1 started to degrade at 55°C and disappeared at 64°C in vehicle-treated cells, whereas it started to degrade at 61°C and disappeared at 70°C in AI-44–treated cells. Furthermore, AI-44 dose-dependently enhanced the level of PRDX1 at 61°C, suggesting the rising stability of PRDX1 with AI-44 treatment (Fig. 4E). These results strongly suggest that PRDX1 is the target protein of AI-44.

AI-44 promotes interaction of PRDX1 with pro-CASP1

We hypothesized that PRDX1 might contribute to NLRP3 inflammasome inactivation by AI-44 treatment. We examined the possible effect of PRDX1 on the formation of the NLRP3 inflammasome complex. Interestingly, reciprocal coimmunoprecipitation assay proved that AI-44 promoted the interaction between PRDX1 and pro-CASP1, whereas the association of ASC and pro-CASP1 was attenuated (Fig. 5A, 5B). Furthermore, confocal immunofluorescence analysis indicated that there was increased colocalization between PRDX1 and pro-CASP1 in macrophages when cells were treated with AI-44 during the process of NLRP3 inflammasome activation (Fig. 5C).

Inhibitory effect of AI-44 on NLRP3 inflammasome activation depends on PRDX1

To further confirm its inhibitory effects on the activation of the NLRP3 inflammasome, PRDX1 was knocked down in THP1 cells using RNA interference. In these PRDX1-knockdown THP1-derived macrophages, the effects of AI-44 on IL-1β secretion and CASP1 activation were examined. On one hand, CASP1 activation was markedly enhanced in the PRDX1-knockdown group compared with the control group (Fig. 6A–C), suggesting PRDX1 is a negative regulator for NLRP3 inflammasome activation. On the other hand, the inhibitory effect of AI-44 on IL-1β production was significantly blocked when PRDX1 was silenced (Fig. 6A). In addition, PRDX1 knockdown also abated the suppressive effect of AI-44 on CASP1 activation as detected by Western blot and flow cytometry assay (Fig. 6B, 6C). It was worth noting that AI-44 did not inhibit reactive oxygen species (ROS) production upon ATP treatment in

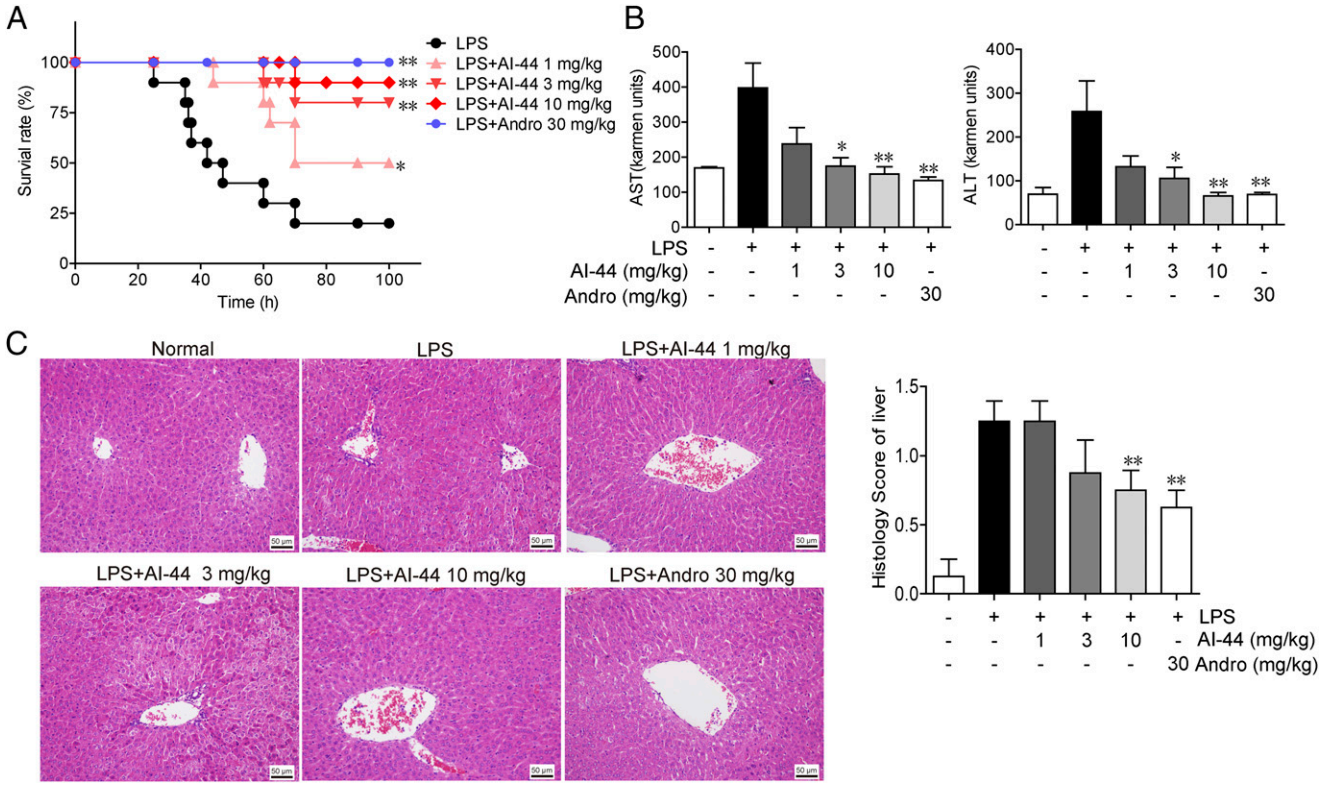

FIGURE 7. Curcumin analogue AI-44 alleviates LPS-induced endotoxemia in mice. (**A**) Mice were i.p. injected with saline vehicle control (LPS alone–treated group), with indicated doses of AI-44, and intragastrically with Andro (positive control) after LPS challenge, and then the survival rates were monitored continuously. (**B** and **C**) After LPS challenge for 24 h, mice were sacrificed. Levels of AST and ALT in serum were measured (B). Representative mouse liver tissue sections were subjected to H&E staining (C). Data are presented as mean ± SEM of 10 mice in each group. $*p < 0.05$, $**p < 0.01$ versus LPS alone–treated group.

macrophage (Supplemental Fig. 2D), suggesting that AI-44–triggered PRDX1-mediated CASP1 inactivation is independent of its antioxidant activity. Our results, in this study, demonstrate that PRDX1 is required for inhibition of the NLRP3 inflammasome by AI-44.

AI-44 alleviates LPS-induced endotoxemia in mice via inhibiting NLRP3 inflammasome activation

To confirm the therapeutic effect of AI-44 on NLRP3 inflammasome–related diseases, an LPS-induced murine endotoxemia model was used in this study. As a result, AI-44 significantly increased the survival rate of septic mice (Fig. 7A). Liver injury caused by LPS was remarkably alleviated in AI-44–treated mice, indicated by decreased levels of ALT and AST in serum (Fig. 7B) and reduced infiltration of the inflammatory cells in liver (Fig. 7C). Overproduction of inflammatory cytokines is thought to be an important reason for the development of severe sepsis. Against this, AI-44 administration inhibited the secretions of proinflammatory cytokines such as IL-1β and IL-6 in serum (Fig. 8A). In addition, infiltration of $CD11b^+$ macrophages was also alleviated by AI-44 (Fig. 8B). Moreover, AI-44 administration markedly suppressed CASP1 activation in peritoneal macrophages isolated from LPS-treated mice (Fig. 8C). The data presented in Figs. 7 and 8 suggested that AI-44 treatment significantly alleviated LPS-induced endotoxemia in mice through inhibiting the NLRP3 inflammasome. It should be noted that NLRP3 knockout dramatically alleviated LPS-induced murine endotoxemia (Supplemental Fig. 4), indicating that NLRP3 contributes to the development of this model. Collectively, these data demonstrate that curcumin analogue AI-44–driven PRDX1 blocks the assembly of the NLRP3 inflammasome, which constitutes a negative regulatory mechanism to limit NLRP3 inflammasome overactivation (Fig. 9).

Discussion

In the current study, we report, to our knowledge, the interaction between PRDX1 and CASP1 in NLRP3 inflammasome regulation for the first time. This interaction, driven by the curcumin analogue AI-44, suppresses the assembly of NLRP3 inflammasome attenuating LPS-induced endotoxemia in mice, suggesting PRDX1 as a negative regulator of the NLRP3 inflammasome and a possible therapeutic target for sepsis and other inflammatory diseases.

The novel function of PRDX1 derived from our study is quite different from its conventional effect on oxidation-reduction regulation. PRDX1 is a member of Prx subfamily, which mainly present in the cytosol. As an antioxidant enzyme, PRDX1 is highly reactive to hydroperoxides, including superoxide, hydrogen peroxide, and the hydroxyl radical, but not to other oxidants or thiol reagents (21). PRDX1 plays an important role in various diseases by involving in many cellular metabolic and signaling processes. In esophageal squamous cell carcinoma, PRDX1 functioned as a tumor suppressor (22), whereas in oral squamous cell carcinoma, PRDX1 was overexpressed and might be a biomarker for the diagnosis and prognosis (23). Additionally, PRDX1 is proven to be essential for antitumor activity of NK cells and antiviral activity of macrophages (24, 25). However, the role of PRDX1 in the NLRP3 inflammasome remains unclear.

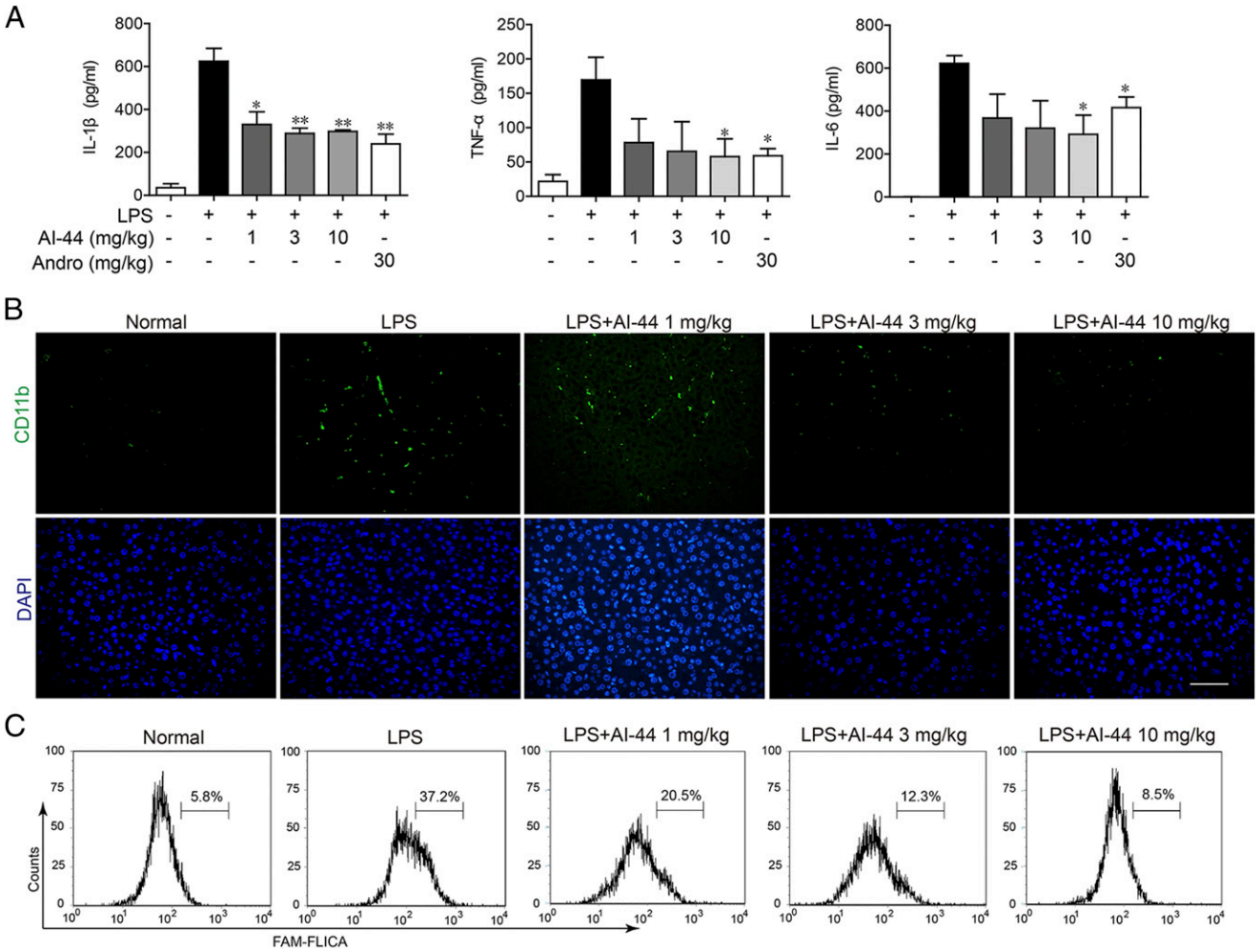

FIGURE 8. Curcumin analogue AI-44 inhibits NLRP3 inflammasome activation in mice with LPS-induced endotoxemia. After LPS challenge for 24 h, mice were sacrificed. (**A**) Levels of proinflammatory cytokines in serum were determined by ELISA. Data are presented as mean ± SEM of 10 mice in each group. $*p < 0.05$, $**p < 0.01$ versus LPS alone–treated group. (**B**) Sections of colonic tissue were immunostained with DAPI (blue) and anti-CD11b–FITC (green) and observed by fluorescence microscope. Scale bar, 50 μm. (**C**) Peritoneal macrophages isolated from mice were stained with FAM FLICA and subjected to flow cytometric analysis. Representative data of three independent experiments are shown in (B and C).

It is well known that mitochondrial dysfunction, exemplified by the overproduction of ROS, is crucial for the signal 2 activation of the NLRP3 inflammasome (9, 26, 27). Detected by DCFH-DA staining, ATP treatment caused a high level of ROS release, but AI-44 hardly inhibited ROS production (Supplemental Fig. 2D), suggesting that the antioxidant activity is dispensable for AI-44–triggered PRDX1-mediated CASP1 inactivation. It is worth pointing out that the function of PRDX1 is not restricted to its antioxidant activity. PRDX1 serves as a molecular chaperon by interacting with APE1 to maintain its protein level and DNA repair activity (28). Moreover, oligomeric PRDX1 directly associates with transcription factor p53 (29), c-Myc (30), NF-κB (31), or androgen receptor (32) in nucleus. In addition, PRDX1 directly or indirectly interacts with several ROS-dependent (redox pathways) effectors, including ASK1, p66Shc, GSTpi/JNK, and c-Abl kinase in cytoplasm (33). Hence, PRDX1 plays important roles in both ROS-dependent and -independent signaling pathways. In the current study, our data suggest that there is a connection between PRDX1 and NLRP3, but the specific role of PRDX1 in NLRP3 inflammasome activation needs further investigation using PRDX1 knockout mice in the future.

Several small molecules have been reported to inhibit NLRP3 inflammasome-dependent IL-1β release without identified target protein. Glyburide acted upstream of NLRP3 and downstream of the P2X7 receptor to block cryopyrin-dependent inflammasome activation by pathogen-associated molecular patterns, damage-associated molecular patterns, and crystalline substances (14). Arsenic trioxide and sodium arsenite induced an altered oxidative state in cells for inhibition of the NLRP3 inflammasome, which was reversed by the ROS scavenger *N*-acetyl-cysteine (34). MCC950, a potent, selective, small-molecule inhibitor of the NLRP3 inflammasome, strongly inhibited canonical and noncanonical NLRP3 activation at nanomolar concentrations with an unknown mechanism (15). Andro was reported to trigger mitophagy, leading to a reversed mitochondrial membrane potential collapse, which in turn inactivated the NLRP3 inflammasome (13). Beyond these findings, our research not only identified a highly potent inhibitor of the NLRP3 inflammasome but also uncovered a new regulator protein for the NLRP3 inflammasome.

In conclusion, our data in this study show that a curcumin analogue, AI-44, alleviates murine sepsis with a possible mechanism of NLRP3 inflammasome inactivation. Using this small compound, we discover a novel regulatory mode in macrophage, in which PRDX1 interacts with CASP1 to interrupt the

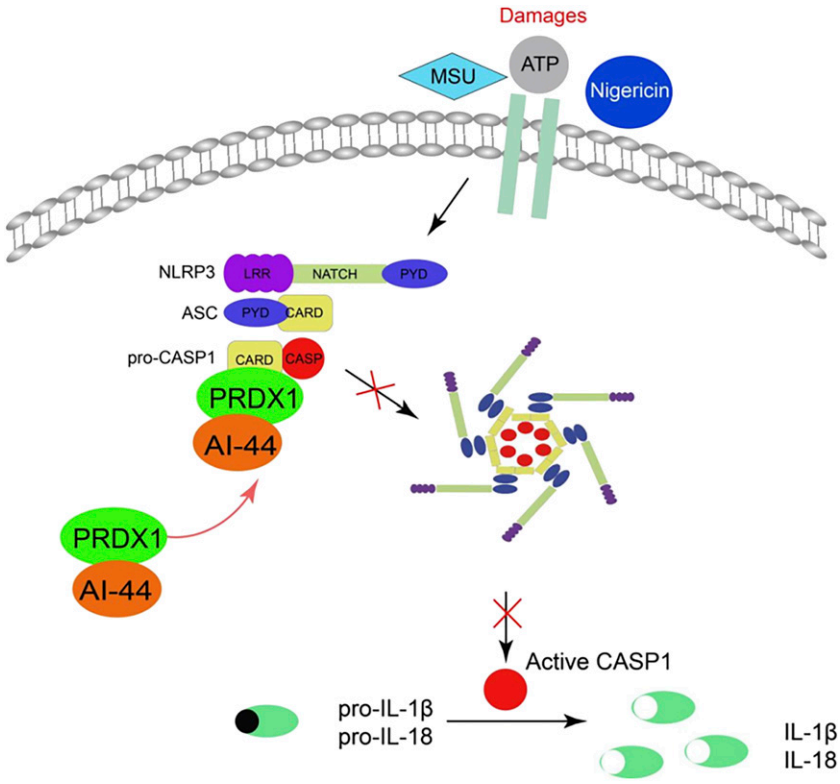

FIGURE 9. The graphic illustration for the mechanism of curcumin analogue AI-44 inhibiting NLRP3 inflammasome activation. NLRP3 inflammasome can be activated by ATP, MSU, or nigericin while small compound AI-44 binds to PRDX1 and promotes the interaction of PRDX1 and pro-CASP1, which leads to suppression of association of pro-CASP1 and ASC. Therefore, the assembly of the NLRP3 inflammasome is blocked, and the activation of CASP1 is inhibited.

assembly of the NLRP3 inflammasome complex. Our findings provide evidence for the possible development of AI-44 as a lead compound for sepsis or other inflammasome-driven inflammatory diseases.

Acknowledgments

We thank Prof. Rongbin Zhou for providing NLRP3$^{-/-}$ mice.

Disclosures

The authors have no financial conflicts of interest.

References

1. Hattori, Y., K. Hattori, T. Suzuki, and N. Matsuda. 2017. Recent advances in the pathophysiology and molecular basis of sepsis-associated organ dysfunction: novel therapeutic implications and challenges. *Pharmacol. Ther.* 177: 56–66.
2. Verdonk, F., A. Blet, and A. Mebazaa. 2017. The new sepsis definition: limitations and contribution to research and diagnosis of sepsis. *Curr. Opin. Anaesthesiol.* 30: 200–204.
3. Jansen, M. J., T. Hendriks, M. T. Vogels, J. W. van der Meer, and R. J. Goris. 1996. Inflammatory cytokines in an experimental model for the multiple organ dysfunction syndrome. *Crit. Care Med.* 24: 1196–1202.
4. Wang, J. E., M. K. Dahle, M. McDonald, S. J. Foster, A. O. Aasen, and C. Thiemermann. 2003. Peptidoglycan and lipoteichoic acid in gram-positive bacterial sepsis: receptors, signal transduction, biological effects, and synergism. *Shock* 20: 402–414.
5. Fry, D. E. 2012. Sepsis, systemic inflammatory response, and multiple organ dysfunction: the mystery continues. *Am. Surg.* 78: 1–8.
6. Sutterwala, F. S., Y. Ogura, M. Szczepanik, M. Lara-Tejero, G. S. Lichtenberger, E. P. Grant, J. Bertin, A. J. Coyle, J. E. Galán, P. W. Askenase, and R. A. Flavell. 2006. Critical role for NALP3/CIAS1/Cryopyrin in innate and adaptive immunity through its regulation of caspase-1. *Immunity* 24: 317–327.
7. Ogura, Y., F. S. Sutterwala, and R. A. Flavell. 2006. The inflammasome: first line of the immune response to cell stress. *Cell* 126: 659–662.
8. Franchi, L., T. Eigenbrod, R. Muñoz-Planillo, and G. Nuñez. 2009. The inflammasome: a caspase-1-activation platform that regulates immune responses and disease pathogenesis. *Nat. Immunol.* 10: 241–247.
9. Nakahira, K., J. A. Haspel, V. A. Rathinam, S. J. Lee, T. Dolinay, H. C. Lam, J. A. Englert, M. Rabinovitch, M. Cernadas, H. P. Kim, et al. 2011. Autophagy proteins regulate innate immune responses by inhibiting the release of mitochondrial DNA mediated by the NALP3 inflammasome. *Nat. Immunol.* 12: 222–230.
10. Wen, H., D. Gris, Y. Lei, S. Jha, L. Zhang, M. T.-H. Huang, W. J. Brickey, and J. P. Y. Ting. 2011. Fatty acid-induced NLRP3-ASC inflammasome activation interferes with insulin signaling. *Nat. Immunol.* 12: 408–415.
11. Allen, I. C., E. M. TeKippe, R. M. Woodford, J. M. Uronis, E. K. Holl, A. B. Rogers, H. H. Herfarth, C. Jobin, and J. P. Ting. 2010. The NLRP3 inflammasome functions as a negative regulator of tumorigenesis during colitis-associated cancer. *J. Exp. Med.* 207: 1045–1056.
12. Dupaul-Chicoine, J., A. Arabzadeh, M. Dagenais, T. Douglas, C. Champagne, A. Morizot, I. G. Rodrigue-Gervais, V. Breton, S. L. Colpitts, N. Beauchemin, and M. Saleh. 2015. The Nlrp3 inflammasome suppresses colorectal cancer metastatic growth in the liver by promoting natural killer cell tumoricidal activity. *Immunity* 43: 751–763.
13. Guo, W., Y. Sun, W. Liu, X. Wu, L. Guo, P. Cai, X. Wu, X. Wu, Y. Shen, Y. Shu, et al. 2014. Small molecule-driven mitophagy-mediated NLRP3 inflammasome inhibition is responsible for the prevention of colitis-associated cancer. *Autophagy* 10: 972–985.
14. Lamkanfi, M., J. L. Mueller, A. C. Vitari, S. Misaghi, A. Fedorova, K. Deshayes, W. P. Lee, H. M. Hoffman, and V. M. Dixit. 2009. Glyburide inhibits the Cryopyrin/Nalp3 inflammasome. *J. Cell Biol.* 187: 61–70.
15. Coll, R. C., A. A. Robertson, J. J. Chae, S. C. Higgins, R. Muñoz-Planillo, M. C. Inserra, I. Vetter, L. S. Dungan, B. G. Monks, A. Stutz, et al. 2015. A small-molecule inhibitor of the NLRP3 inflammasome for the treatment of inflammatory diseases. *Nat. Med.* 21: 248–255.
16. Guo, W., W. Liu, Z. Chen, Y. Gu, S. Peng, L. Shen, Y. Shen, X. Wang, G. S. Feng, Y. Sun, and Q. Xu. 2017. Tyrosine phosphatase SHP2 negatively regulates NLRP3 inflammasome activation via ANT1-dependent mitochondrial homeostasis. *Nat. Commun.* 8: 2168.
17. Jin, J., Q. Yu, C. Han, X. Hu, S. Xu, Q. Wang, J. Wang, N. Li, and X. Cao. 2013. LRRFIP2 negatively regulates NLRP3 inflammasome activation in macrophages by promoting Flightless-I-mediated caspase-1 inhibition. *Nat. Commun.* 4: 2075.
18. Bruchard, M., G. Mignot, V. Derangère, F. Chalmin, A. Chevriaux, F. Végran, W. Boireau, B. Simon, B. Ryffel, J. L. Connat, et al. 2013. Chemotherapy-triggered cathepsin B release in myeloid-derived suppressor cells activates the Nlrp3 inflammasome and promotes tumor growth. *Nat. Med.* 19: 57–64.
19. Martinez Molina, D., R. Jafari, M. Ignatushchenko, T. Seki, E. A. Larsson, C. Dan, L. Sreekumar, Y. Cao, and P. Nordlund. 2013. Monitoring drug target engagement in cells and tissues using the cellular thermal shift assay. *Science* 341: 84–87.
20. Liu, W., W. Guo, J. Wu, Q. Luo, F. Tao, Y. Gu, Y. Shen, J. Li, R. Tan, Q. Xu, and Y. Sun. 2013. A novel benzo[d]imidazole derivate prevents the development of dextran sulfate sodium-induced murine experimental colitis via inhibition of NLRP3 inflammasome. *Biochem. Pharmacol.* 85: 1504–1512.
21. Alegria, T. G., D. A. Meireles, J. R. Cussiol, M. Hugo, M. Trujillo, M. A. de Oliveira, S. Miyamoto, R. F. Queiroz, N. F. Valadares, R. C. Garratt, et al. 2017. Ohr plays a central role in bacterial responses against fatty acid hydroperoxides and peroxynitrite. *Proc. Natl. Acad. Sci. USA* 114: E132–E141.
22. Hoshino, I., H. Matsubara, Y. Akutsu, T. Nishimori, Y. Yoneyama, K. Murakami, H. Sakata, K. Matsushita, and T. Ochiai. 2007. Tumor suppressor Prdx1 is a

prognostic factor in esophageal squamous cell carcinoma patients. *Oncol. Rep.* 18: 867–871.
23. Lee, E. Y., J. Y. Kang, and K. W. Kim. 2015. Expression of cyclooxygenase-2, peroxiredoxin I, peroxiredoxin 6 and nuclear factor-κB in oral squamous cell carcinoma. *Oncol. Lett.* 10: 3129–3136.
24. Siernicka, M., M. Winiarska, M. Bajor, M. Firczuk, A. Muchowicz, M. Bobrowicz, C. Fauriat, J. Golab, D. Olive, and R. Zagozdzon. 2015. Adenanthin, a new inhibitor of thiol-dependent antioxidant enzymes, impairs the effector functions of human natural killer cells. *Immunology* 146: 173–183.
25. Matsumura, K., H. Iwai, M. Kato-Miyazawa, F. Kirikae, J. Zhao, T. Yanagawa, T. Ishii, T. Miyoshi-Akiyama, K. Funatogawa, and T. Kirikae. 2016. Peroxiredoxin 1 contributes to host defenses against *Mycobacterium tuberculosis*. *J. Immunol.* 197: 3233–3244.
26. Zhou, R., A. S. Yazdi, P. Menu, and J. Tschopp. 2011. A role for mitochondria in NLRP3 inflammasome activation. [Published erratum appears in 2011 *Nature* 475: 122.] *Nature* 469: 221–225.
27. Gurung, P., J. R. Lukens, and T. D. Kanneganti. 2015. Mitochondria: diversity in the regulation of the NLRP3 inflammasome. *Trends Mol. Med.* 21: 193–201.
28. Nassour, H., Z. Wang, A. Saad, A. Papaluca, N. Brosseau, B. Affar el, M. A. Alaoui-Jamali, and D. Ramotar. 2016. Peroxiredoxin 1 interacts with and blocks the redox factor APE1 from activating interleukin-8 expression. *Sci. Rep.* 6: 29389.
29. Morinaka, A., Y. Funato, K. Uesugi, and H. Miki. 2011. Oligomeric peroxiredoxin-I is an essential intermediate for p53 to activate MST1 kinase and apoptosis. *Oncogene* 30: 4208–4218.
30. Egler, R. A., E. Fernandes, K. Rothermund, S. Sereika, N. de Souza-Pinto, P. Jaruga, M. Dizdaroglu, and E. V. Prochownik. 2005. Regulation of reactive oxygen species, DNA damage, and c-Myc function by peroxiredoxin 1. *Oncogene* 24: 8038–8050.
31. Hansen, J. M., S. Moriarty-Craige, and D. P. Jones. 2007. Nuclear and cytoplasmic peroxiredoxin-1 differentially regulate NF-kappaB activities. *Free Radic. Biol. Med.* 43: 282–288.
32. Park, S. Y., X. Yu, C. Ip, J. L. Mohler, P. N. Bogner, and Y. M. Park. 2007. Peroxiredoxin 1 interacts with androgen receptor and enhances its transactivation. *Cancer Res.* 67: 9294–9303.
33. Ding, C., X. Fan, and G. Wu. 2017. Peroxiredoxin 1 - an antioxidant enzyme in cancer. *J. Cell. Mol. Med.* 21: 193–202.
34. Maier, N. K., D. Crown, J. Liu, S. H. Leppla, and M. Moayeri. 2014. Arsenic trioxide and other arsenical compounds inhibit the NLRP1, NLRP3, and NAIP5/NLRC4 inflammasomes. *J. Immunol.* 192: 763–770.